

A sliding mode multimodel control for a sensorless photovoltaic system

Ahmed Rhif, Zohra Kardous and Naceur BenHadj Braiek

Advanced System Laboratory, Polytechnic School of Tunisia (Laboratoire des Systèmes Avancés(LSA), Ecole Polytechnique de Tunisie, BP 743, 2078 La Marsa, Tunisie

Received 19 December 2011; revised 24 April 2012; accepted 02 May 2012

This study presents a sliding mode multimodal control for a sensorless photovoltaic panel, which sets itself as per the sun position at every second during the day for a period of five years; then tracker, using sliding mode multimodal controller and a sliding mode observer, will track these positions to make sunrays orthogonal to photovoltaic cell that produces more energy. After sunset, tracker goes back to initial position of sunrise. This autonomic dual axis sun tracker increases power production by over 40%.

Keywords: Altitude, Azimuth, Photovoltaic panel, Solar energy, Sun tracker

Introduction

Photovoltaic arrays are fixed. In this way, solar energy incident on modules is not optimal during time variation and seasons. Theoretical studies¹⁻² show that energy supplied by a photovoltaic cell equipped by a sun tracker (ST) is higher (30-40%) than energy provided by fixed panels (Fig. 1). A solar panel (3 m²) fixed to a surface produces 5 kWh of electricity per day. The same installation, if equipped with a tow axis sun ST³⁻⁵ (Fig. 2), can provide up to 8 kWh per day. This study presents speed and position control of ST using sliding mode control (SMC) and a sliding mode observer (SMO).

Experimental Section

Dual Axis Sun Tracker (ST) Modelling

A dual-axis tracking system with two degrees of freedom (DOF) was used for following the sun position in both altitude and azimuth directions, keeping the sun's rays normal to photovoltaic cell. Operational subset of ST has two DOF, motorized by tow stepper motors, in order to track exactly the prescribed sun's path. Mechanical system (Fig. 3) consists of altitude motor to drive horizontal axis, azimuth motor to drive vertical axis and photovoltaic cell (150 mm x 100 mm). It was designed using solidWorks software in the Department of Electronics, High Institute of Applied Sciences and

Technologies Sousse (ISSAT so), and realised in Plexiglas profiles in order to obtain a simple and economic structure.

Considering that system operation is accomplished by one of those stepper motors at each time, mathematical model of the process in d-q (direct-quadrature) transformation⁶ (Fig. 4) would be given as

$$\begin{cases} \frac{di_d}{dt} = \frac{1}{L}(v_d - Ri_d + NL\Omega i_q) \\ \frac{di_q}{dt} = \frac{1}{L}(v_q - Ri_q + NL\Omega i_d - K\Omega) \\ \frac{d\Omega}{dt} = \frac{1}{J}(Ki_q - f_v\Omega - C) \\ \frac{dq}{dt} = \Omega \end{cases} \dots(1)$$

where R , resistance; L inductance, J , inertia; N , spin number; K , torque constant gain; f_v , friction; Ω , angular velocity; q , rotor position; i_d and i_q , currents in d-q referential; and v_d and v_q , voltages in d-q referential.

Considering $\begin{cases} x = [i_d, i_q, q, \Omega]^T \\ u = [v_d, v_q]^T \end{cases}$, then model state

function will be given as

$$\dot{x} = f(\Omega)x + gu + p \dots(2)$$

*Author for correspondence
 E-mail: ahmed.rhif@gmail.com

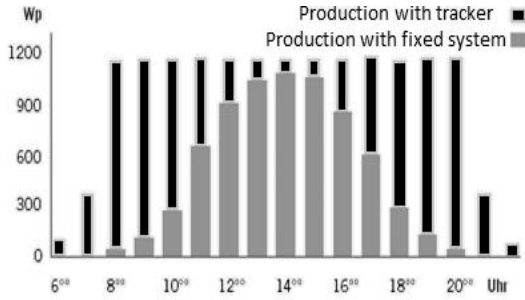


Fig.1—Histogram of solar energy produced



Fig.2—Two axis system orientation

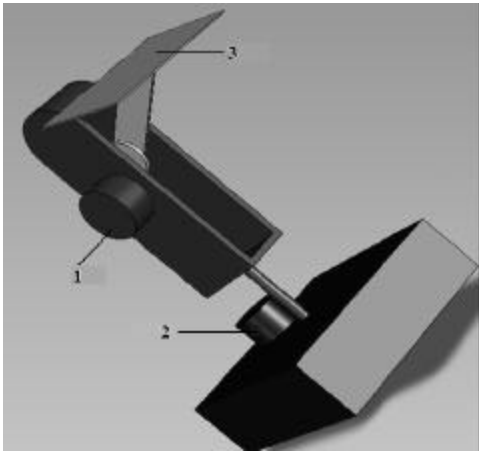


Fig. 3—Mechanical design of the process

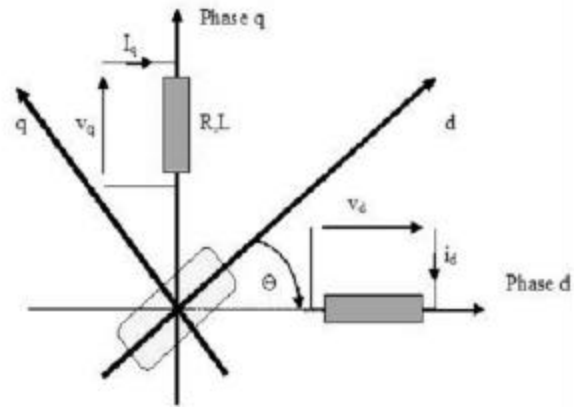


Fig.4—Electrical model in d-q referential

where

$$f(\Omega) = \begin{bmatrix} -\frac{R}{L} & N\Omega & 0 & 0 \\ N\Omega & -\frac{R}{L} & a_{23} & -K \\ 0 & 0 & 0 & 1 \\ 0 & \frac{K}{J} & 0 & -\frac{f_v}{J} \end{bmatrix} \quad g = \begin{bmatrix} \frac{1}{L} & 0 \\ 0 & \frac{1}{L} \\ 0 & 0 \\ 0 & 0 \end{bmatrix} \quad p = \begin{bmatrix} 0 \\ 0 \\ 0 \\ -\frac{C}{J} \end{bmatrix} \quad \text{with}$$

f and g as linear functions.

In other way, Eq. (2) could be given in a simplest way; considering $y_1 = \mathbf{q}$ and $y_2 = i_d$, Eq. (1) gives

$$\begin{cases} \mathbf{q} = y_1 \\ \Omega = \dot{y}_1 \\ i_d = y_2 \\ i_q = \frac{1}{K}(J\ddot{y}_1 + f_v\dot{y}_1 + C) \\ v_d = L\dot{y}_2 + Ry_2 - \frac{NL}{K}\dot{y}_1(J\ddot{y}_1 + f_v\dot{y}_1 + C) \\ v_q = \frac{JL}{K}y_1^{(3)} + \frac{1}{K}(Lf_v + RJ)\ddot{y}_1 + \left(\frac{Rf_v}{K} + K + NLy_2\right)\dot{y}_1 + \frac{L}{K}\dot{C} \end{cases} \dots(3)$$

Controller Designs

Among controller types tested and implemented in ST, Hua & Shen¹ compared sun tracking effectiveness of maximum power point tracking (MPPT) algorithms with a control method, which combined a discrete control and a Proportional Integral (PI) controller to track maximum power points of a solar array⁷⁻¹⁰. Yousef¹¹ developed a ST system with a fuzzy logic control for nonlinear dynamics of tracking mechanism^{12,13}. Roth¹⁴ designed a solar tracking system to measure direct solar radiation. The system was controlled by a closed loop servo system composed by four quadrant photo-detectors needed to sense the position of sun^{15,16}. Finally, a sensorless control test using SMC, which is very solicited in tracking path studies.

High Order Sliding Mode Control (SMC)

SMC can bring back the system state on sliding surface, where it will slide along the desired state. However, SMC needs a high level of discontinuous control, which makes harmful effects on actuators, known as chattering phenomenon (CP). As a solution, designing

of a high order SMC consists of sliding variable derivative computing¹⁷⁻²². A second order SMC consists of $s(x) = \dot{s}(x) = 0$ and $\dot{V} = \frac{1}{2} \frac{\partial}{\partial t} (s^2) = s\dot{s} \leq -h|s|$ with $h > 0$ and V as Lyapunov quadratic function. Path tracking error in the origin is stabilized as $e = [i_d - i_{dr}, i_q - i_{qr}, \Omega - \Omega_r, \mathbf{q} - \mathbf{q}_r]^T = [e_1, e_2, e_3, e_4]^T$. Using Eq. (1), one gets

$$\begin{cases} \dot{e}_1 = \frac{1}{L}(v_d - v_{dr} - Re_1 + NL(e_3e_2 + e_3i_{qr} + e_2\Omega_r)) \\ \dot{e}_2 = \frac{1}{L}(v_q - v_{qr} - Re_2 + NL(e_3e_1 + e_3i_{dr} + e_1\Omega_r) - Ke_3) \\ \dot{e}_3 = \frac{1}{J}(Ke_2 - f_v e_3 - C_r) \\ \dot{e}_4 = e_3 \end{cases} \dots(4)$$

where e , system error; i_{dr} & i_{qr} , reference current in d-q referential; v_{dr} & v_{qr} , reference voltage in d-q referential, Ω_r reference angular velocity; and \mathbf{q}_r , reference rotor position.

For velocity control by a second order SMC, sliding surface is written as $s_\Omega = \mathbf{m}e_3 + \dot{e}_3$ with $\mathbf{m} > 0$. First order derivative of Eq. (4) gives $\dot{s}_\Omega = \mathbf{m}\dot{e}_3 + \ddot{e}_3$ and $\dot{s}_\Omega = \mathbf{m} \frac{1}{J}(Ke_2 - f_v e_3 - C_r) + \frac{1}{J}(Ke_2 - f_v \dot{e}_3 - \dot{C}_r)$. In second phase, to deal with position control process, sliding surface is considered as

$$s_q = \mathbf{m}_1 e_4 + \mathbf{m}_2 \dot{e}_4 + \ddot{e}_4 \dots(5)$$

Combining Eq. (4) and Eq. (5) gives $s_q = \mathbf{m}_1 e_4 + \mathbf{m}_2 e_3 + \frac{1}{J}(Ke_2 - f_v e_3 - C_r)$ with $\mathbf{m}_1, \mathbf{m}_2 > 0$. In convergence phase, to bring the system on sliding surface, different forms of switching control are available. In this study, the following were chosen ($U_0 > 0$): $u_{s1} = -U_0 \text{sign}(s_\Omega)$; and $u_{s2} = -U_0 \text{sign}(s_q) = \dot{s}_q$.

Proposed Sliding Mode Multimodel Control (SM-MMC) Synthesis

Multimodel approach represents an interesting alternative to SMC problems, and a powerful tool for identification, control and analysis of complex systems. Multimodel principle makes possible the design of a non linear control composed by linear sub controls relative to each sub model. The process control could be then deduced from a fusion or a commutation between different partial controls weighted by equivalent validities. In this sense, several methods of validities estimation

[$v_{in}(t) = \frac{v_i(t)}{\sum_{i=1}^N v_i(t)}$ and $v_i(t) = 1 - r_{in}(t)$] are already reported. These methods are classified according to the models acquisition ways, which are related to process knowledge. This paper will apt for residue approach for validities computing as

$$r_{in}(t) = \frac{r_i(t)}{\sum_{i=1}^N r_i(t)} \dots(6)$$

$$r_i(t) = |y(t) - y_i(t)| ; i= 1, \dots, N \dots(7)$$

where v_i , validity; r_i , residue; $y(t)$, system's output; and $y_i(t)$, output of i^{th} model.

In order to reduce disturbances due to inadequate models, validities were reinforced as

$$v_i^{ref}(t) = v_i(t) \prod_{\substack{j=1 \\ i \neq j}}^N (1 - v_j(t)) \dots(8)$$

Normalized reinforced validities are given as

$$v_{in}^{ref}(t) = \frac{v_i^{ref}(t)}{\sum_{i=1}^N v_i^{ref}(t)} \dots(9)$$

SM-MMC uses multimodel fusion approach to reduce switching control effect, which induces CP²³⁻²⁴. To improve control performances, Ure & Inalhan²⁵ applied a discrete sliding mode. In another study²⁶, a non linear control was considered for a combat air vehicle to execute agile manoeuvres. To reduce CP, fuzzy mode was applied to a high fidelity six degrees of freedom F-16 fighter aircraft model. In this study, control approach consisted in carrying out a fusion on sliding mode discontinuous control (Fig. 2) to eliminate or minimize CP. To adapt the controlling process to each sub model, several sliding surfaces were used, each state of a sub model M_i was considered to reach one of these sliding surfaces s_i (Fig. 5). To ensure SMC existence, several switching control u_{si} relative to each sliding surface s_i were used. Then, partial controls y_i of each sub model will contribute on validities calculationas

$$u_{si} = \begin{cases} u_{si \min} & si \quad \text{sign}(s) < 0 \\ u_{si \max} & si \quad \text{sign}(s) > 0 \end{cases} \dots(10)$$

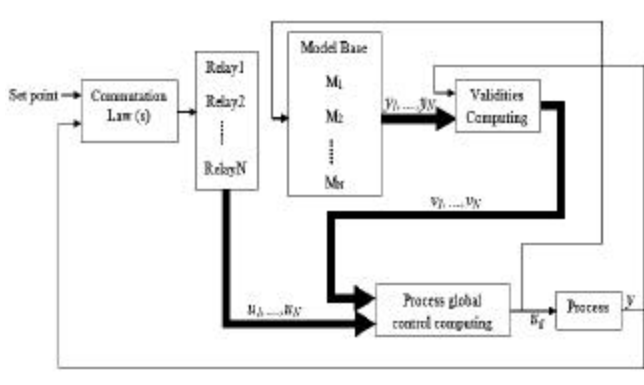


Fig.5—Sliding mode multimodel control (SM-MMC) structure

After that, process will converge to the sum of those surfaces weighted by correspondent validities $u_i (S = \sum_i u_i s_i)$ and global control will be obtained by adding partials controls $u_i (u_i = u_{ei} + u_{si})$ weighted by adapted validities computed on line ($u_g = \sum_{i=1}^N n_i u_i$) with u_{ei} , equivalent control relative to each sliding surface. In this way, to improve performances of this control, a PID sliding surface²⁷⁻²⁸ was used, and designed as

$$s_i = a_i(x_d - x_r) + b_i \frac{d(x_d - x_r)}{dt} + g_i \int_0^t (x_d - x_r) dt \quad \dots(11)$$

$$\text{Then, } \dot{s}_i = a_i \frac{d(x_d - x_r)}{dt} + b_i \frac{d^2(x_d - x_r)}{dt^2} + g_i (x_d - x_r)$$

with $a_i, b_i, g_i > 0, i=1, \dots, N, x_d$ the desired state and x_r the real state. To reduce CP, saturation function was used to give

$$u_{si} = I_i \text{sat} \left(\frac{s_i}{\Psi_i} \right) \quad \dots(12)$$

where

$$u_{si} = \begin{cases} I_i \text{sign}(s_i) & \text{if } |s_i| \geq \Psi_i \\ I_i \left(\frac{s_i}{\Psi_i} \right) & \text{if } |s_i| \leq \Psi_i \end{cases} \quad \dots(13)$$

with I_i and $\Psi_i > 0, \Psi$ defines the boundary layer thickness.

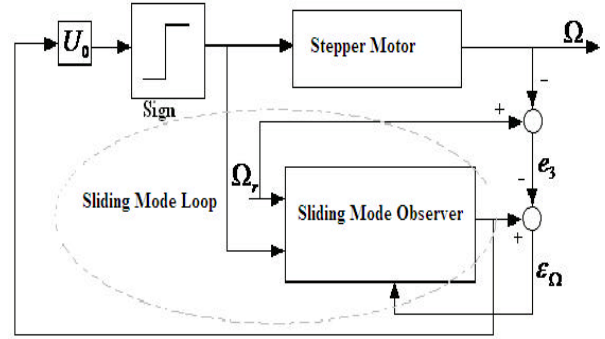


Fig.6—Velocity control based on a sliding mode observer (SMO)

Sliding Mode Observer (SMO)

Angular velocities of stepper motors measurements could give unreliable results because of disturbances that influence tachymetry sensor. Therefore, angular velocity Ω is estimated using SMO instead of sensor. This operation would give better results and will reduce the number of sensors, which are very costly and may have hard maintenance skills. SMO can be used in the state observers design, and has the ability to bring coordinates of estimator error dynamics to zero in finite time. SMOs (Fig. 6) have attractive measurement noise resilience, which is similar to a Kalman filter. CP concerned with sliding mode method can be eliminated by modifying SMO gain, without sacrificing the control robustness and precision qualities²⁹⁻³⁴.

Observed position error is given as $e_q = q - \hat{q}$ and angular velocity error as $e_\Omega = \Omega - \hat{\Omega}$, with \hat{q} estimated position and $\hat{\Omega}$ estimated angular velocity. Angular velocity is equal to the position derivative as $\dot{e}_q = \frac{dq}{dt} - \frac{d\hat{q}}{dt} = \Omega - \hat{\Omega} = e_\Omega$. In this case, Eq. (1) could be represented as

$$\begin{cases} \frac{d\hat{\Omega}}{dt} = \frac{K}{J} i_q - \frac{f_v}{J} \hat{\Omega} - \frac{C_r}{J} + I_2 \text{sign}(\Omega - \hat{\Omega}), & \text{with } I_1, I_2 > 0 \\ \frac{d\hat{q}}{dt} = \hat{\Omega} + I_1 \text{sign}(q - \hat{q}) \end{cases} \quad \dots(14)$$

and

$$\begin{cases} \dot{e}_q = e_\Omega - I_1 \text{sign}(e_q) \\ \dot{e}_\Omega = \frac{d\Omega}{dt} - \frac{d\hat{\Omega}}{dt} = -\frac{f_v}{J} e_\Omega \end{cases} \quad \dots(15)$$

To ascertain state converge to sliding surface, one has to verify Lyapunov²⁶⁻²⁹ stability criterion given by

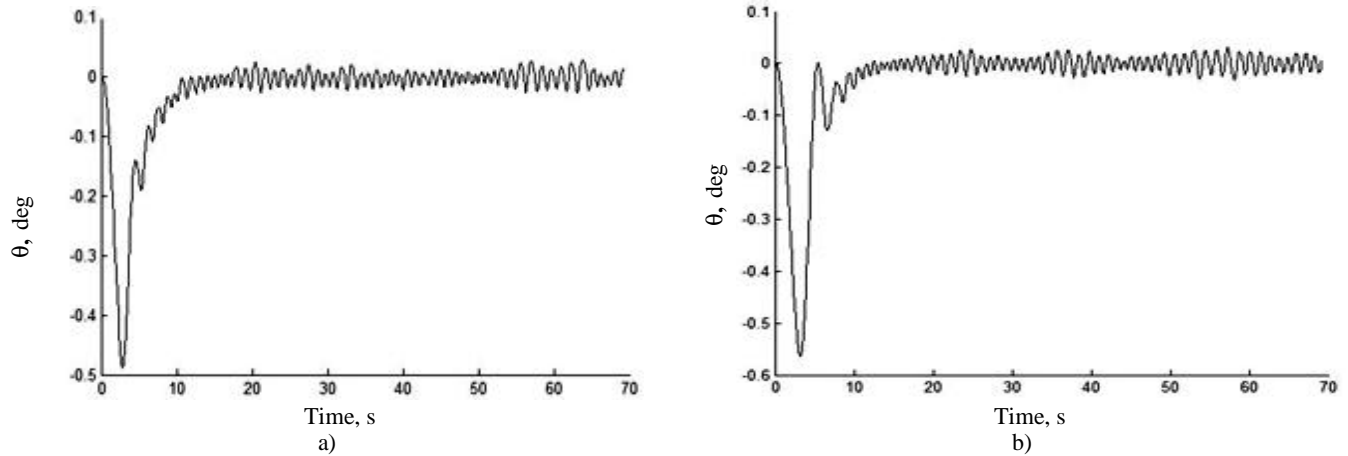


Fig.7—Inclination angle using sliding mode control (SMC) of: a) azimuth motor; and b) altitude motor

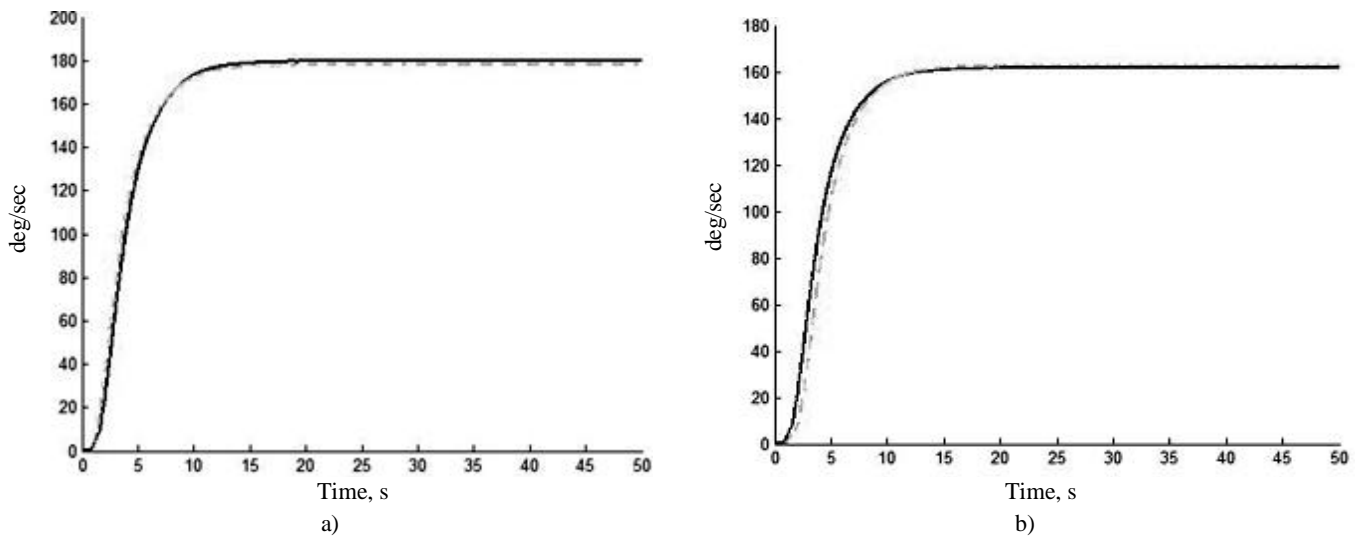


Fig. 8—Real and observed angular velocity of: a) azimuth motor; and b) altitude motor

quadratic function $V_1 = \frac{1}{2} \mathbf{e}_q^2$. In this way, $\dot{V}_1 = \mathbf{e}_q (\mathbf{e}_\Omega - I_1 \text{sign}(\mathbf{e}_q))$. Then, $\dot{V}_1 < 0$ if $I_1 > |\mathbf{e}_\Omega|_{\max}$ and system dynamic is given by $\mathbf{e}_\Omega = I_1 \text{sign}(\mathbf{e}_q)$ when $\mathbf{e}_q \rightarrow 0$. Consider now a second Lyapunov quadratic function $V_2 = \frac{1}{2} (\mathbf{e}_q^2 + J \mathbf{e}_\Omega^2)$. As $\mathbf{e}_q = 0$, Eq. (7) gives $\dot{V}_2 = -f_v \mathbf{e}_\Omega^2 - \mathbf{e}_\Omega (I_2 \text{sign}(\mathbf{e}_\Omega) - C_r)$, then $\dot{V}_2 < 0$ if $I_2 > |C_r|_{\max}$.

Results and Discussion

Experimental results were accomplished for a second order SMC of Eq. (2) applied on the system (Fig. 3) connected to a computer through a serial cable RS232. This required system control evolution, real and observed angular velocities, Ω_1 and Ω_2 , and azimuth and altitude inclinations, θ_1 and θ_2 . Sliding surface parameters used were $\mathbf{n} = 0.135$, $\mathbf{m}_1 = 1.2$ and $\mathbf{m}_2 = 0.355$. Stepper motor

characteristics were as follows: inertia moment J, 3.0145 10^{-4}kg.m^2 ; mechanical torque C, 0.780 Nm; torque constant K, 0.433 Nm/A; armature resistance R, 3.15 Ohm; armature inductance L, 8.15 mH; and friction forces f_v , 0.0172 Nms/rad. Experimental test was considered for time exceeding 100 s.

Using second order SMC, it was observed (Fig. 7) that steady state is reached in a short time (~15 s). Also, for the first test, $\theta_1 = 0.48^\circ$ and $\theta_2 = 0.57^\circ$; thus azimuth inclination θ_1 is very close to altitude inclination θ_2 . This fact is related to elliptic movement nature of sun. However, presence of CP (~0.01°) was noticed. Real and observed angular velocities (Fig. 8) of two axis tracker are very close; $\Omega_1 = 180^\circ/\text{s} \approx \hat{\Omega}_1$ and $\Omega_2 = 160^\circ/\text{s} \approx \hat{\Omega}_2$. This excellent result is due to high estimation quality of SMO. Moreover, SMC shows its robustness (Fig. 7)

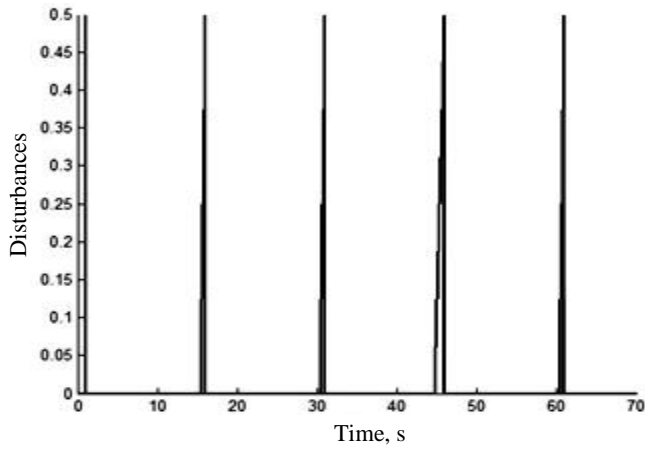


Fig.9—Disturbance signal

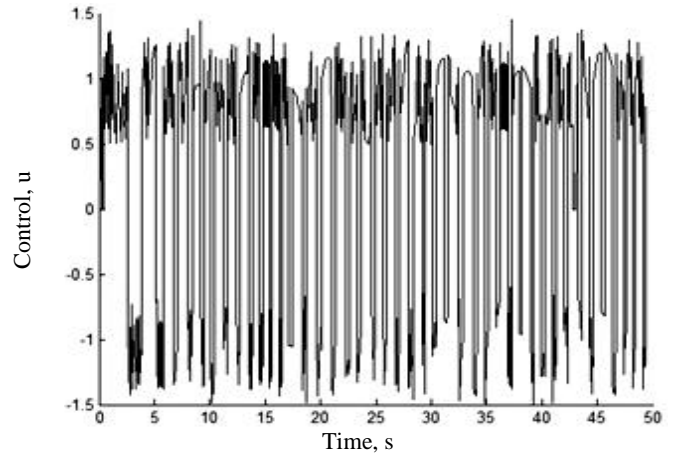
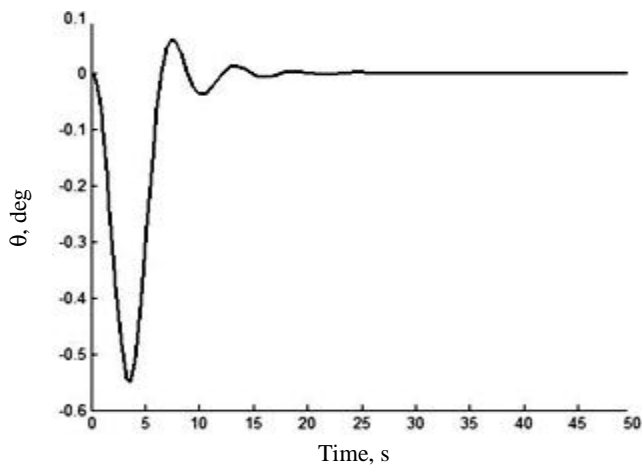
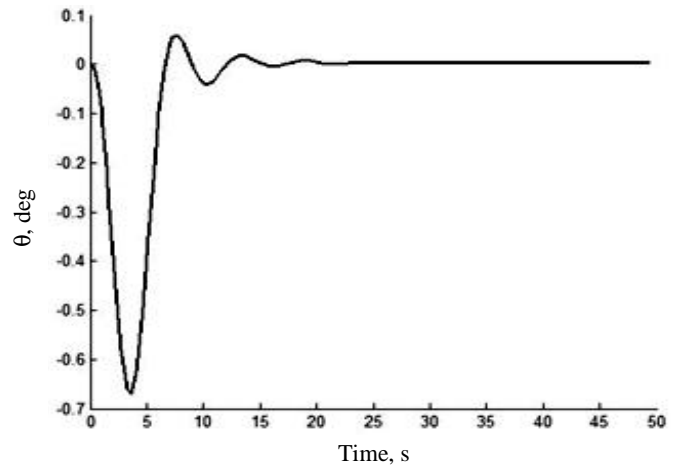


Fig.10—SMC evolution



a)



b)

Fig.11—Inclination angle using SM-MMC of: a) azimuth motor; and b) altitude motor

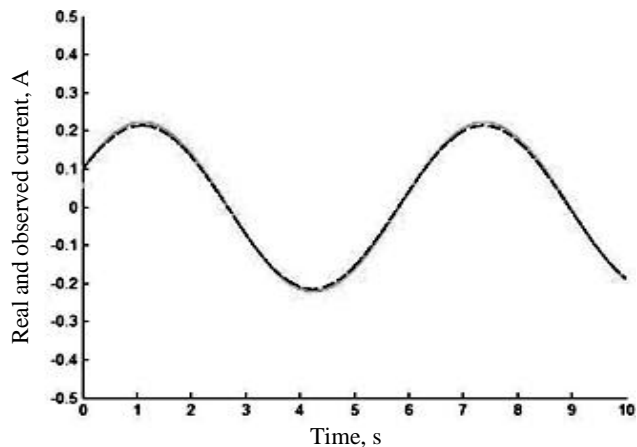


Fig. 12—Real and observed current of the control

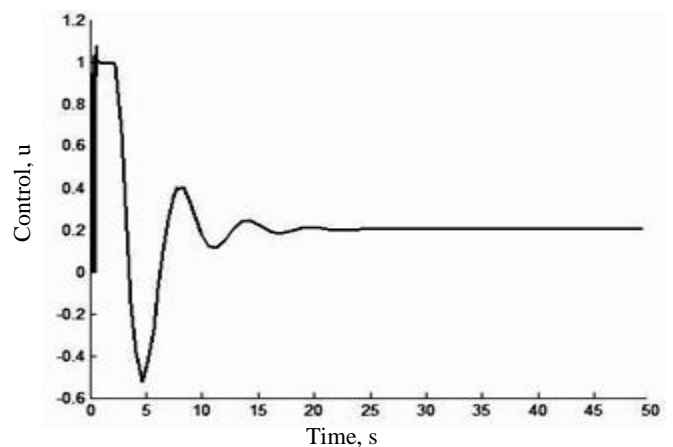


Fig.13—SM-MMC evolution

when a periodic disturbance signal is injected (Fig. 9) with a signal period T of 15 s. System does not deviate from trajectory and preserve its equilibrium position. However, control evolution (Fig. 10), with no high level but with sharp commutations frequency, does not give

adequate operating conditions for actuators (both azimuth and altitude motors). As a solution to these problems (chattering and control oscillations), system was simulated by PID SM-MMC approach, resulting in CP elimination (Fig. 11). Also, control evolution (Figs 12 & 13) of the

system had less commutation frequency and reached steady state in a very short time, which preserved robustness of the system and gave good conditions for actuators.

Conclusions

In this study a SMO has been considered to evaluate angular velocities of stepper motors. Experimental results showed effectiveness of SMC in tracking process and its robustness unless disturbances and high estimation quality of SMO. PID SM-MMC was designed and process simulated. This new approach showed excellent result in term of CP elimination and control stabilization with preserving control robustness.

References

- 1 Hua C & Shen C, Comparative study of peak power tracking techniques for solar storage system, in *IEEE Appl Power Electron Conf & Expo* (Anaheim, CA, USA) 15-19 Feb 1998.
- 2 Lee D S & Youn M J, Controller design of variable structure systems with nonlinear sliding surface, *Electron Lett*, **25** (1989) 1715-1716.
- 3 Rhif A, Position control review for a photovoltaic system: dual axis sun tracker, *IETE Tech Rev*, **28** (2011) 479-485.
- 4 Semma R P & Imamura M S, Sun tracking controller for multi-kW photovoltaic concentrator system, in *Proc 3rd Int Photovoltaic Sol Energy Conf* (Cannes, France) 1980, 27-31.
- 5 McFee R H, Power collection reduction by mirror surface non flatness and tracking error for a central receiver solar power system, *Appl Opt*, **14** (1975) 1493-1502.
- 6 Nollet F, *lois de commande par mode glissants du moteur pas à pas*, thesis, l'Ecole Centrale de Lille et l'Université des Sciences et Technologies de Lille, 2006.
- 7 Singh B & Rajagopal V, Decoupled solid state controller for asynchronous generator in pico-hydro power generation, *IETE J Res*, **56** (2010) 139-150.
- 8 Singh B & Kasal G, An improved electronic load controller for an isolated asynchronous generator feeding 3-phase 4-wire loads, *IETE J Res*, **54** (2008) 244-254.
- 9 Hernandez-Martinez E O, Medina A & Olguin-Salinas D, Fast time domain periodic steady-state solution of nonlinear electric networks containing DVRs, *IETE J Res*, **57** (2011) 105-110.
- 10 Rhif A, Stabilizing sliding mode control design and application for a DC motor: speed control, *Int J Instrum Cont Syst (IJICS)*, **2** (2012) 25-33.
- 11 Yousef H A, Design and implementation of a fuzzy logic computer-controlled sun tracking system, in *IEEE Int Symp Ind Electron* (Bled, Slovenia) 12-16 July 1999.
- 12 Hanmandlu M, AI based governing technique for automatic control of small hydro power plants, *IETE J Res*, **53** (2007) 119-126.
- 13 Singh M, Srivastava S & Gupta J R P, Identification and control of nonlinear system using neural networks by extracting the system dynamics, *IETE J Res*, **53** (2007) 43-50.
- 14 Roth P, Georgieg A & Boudinov H, Design and construction of a system for sun-tracking, *Renew Energ*, **29** (2004) 393-402.
- 15 Hsieh S P, Hwang T S & Ni C W, Twin VCM controller design for the nutator system with evolutionary algorithm, *IETE Tech Rev*, **26** (2009) 290-302.
- 16 Kamath S, George V I & Vidyasagar S, Simulation study on closed loop control algorithm of type 1 diabetes mellitus patients, *IETE J Res*, **55** (2009) 230-235.
- 17 Rhif A, A sliding mode control for a sensorless tracker: application on a photovoltaic system, *Int J Cont Theory Compu Modelling (IJCTCM)*, **2** (2012) 1-14.
- 18 Rhif A, Kardous Z & Ben Hadj Braiek N, A high order sliding mode-multimodel control of non linear system simulation on a submarine mobile, in *Int Multi-Conf on Syst, Signals & Devices (SSD'11)* (Tunisia,) 14-19 March 2011.
- 19 Rhif A, A review note for position control of an autonomous underwater vehicle, *IETE Tech Rev*, **28** (2011) 486-492,.
- 20 Sellami A, Andoulsi R, Mhiri R & Ksouri M, *Sliding Mode Control Approach for MPPT of a Photovoltaic Generator coupled to a DC Water Pump* (JTEA, Sousse) 2002.
- 21 Anosov D V, On stability of equilibrium points of relay systems, *Automat Remote Cont*, **2** (1959) 135-139.
- 22 Utkin V I, Variable structure systems with sliding modes, *IEEE Trans Automat Cont*, **22** (1977) 212-222.
- 23 Rhif A, Kardous Z & Ben Hadj Braiek N, First and high order sliding mode-multimodel stabilizing control synthesis by a single and multi sliding surfaces of nonlinear systems simulation on a submarine mobile, *Trans Syst, Signals Devices*, 2012 (in press).
- 24 Rhif A, Kardous Z & Ben Hadj Braiek N, Stabilizing sliding mode-multimodel control for nonlinear systems simulation on an aircraft: airbus A340, in *Int Multi-Conf on Syst, Signals & Devices (SSD'12)* (Germany,) 2012.
- 25 Kemal Ure N & Inalhan G, *Design of Higher Order Sliding Mode Control Laws for a Multi Modal Agile Maneuvering DCAV* (IEEE, Turkey) 2008.
- 26 Li Z & Shui-sheng Q, Analysis and experimental study of proportional-integral sliding mode control for DC/DC converter, *J Electron Sci Technol China*, **3** (2005).
- 27 Rhif A, A high order sliding mode control with PID sliding surface: Simulation on a Torpedo, *Int J Inform Technol, Cont & Automat (IJITCA)*, **2** (2012) 1-13.
- 28 Rhif A, A sliding mode control with a PID sliding surface for power output maximizing of a wind turbine, *J Instrum Cont*, **2** (2012) 11-16.
- 29 Rhif A, Kardous Z & Ben Hadj Braiek N, A high order sliding mode observer: Torpedo guidance application, *J Engg Technol*, **2** (2012) 13-18.
- 30 Alaybeyoglu A, Erciyas K, Kantarci A & Dagdeviren O, Tracking fast moving targets in wireless sensor networks, *IETE Tech Rev*, **27** (2010) 46-53.
- 31 Petrellis N, Konofaos N & Ph Alexiou G, Estimation of a target position based on infrared pattern reception quality, *IETE Tech Rev*, **27** (2010) 36-45.
- 32 Flota M, Alvarez-Salas R, Miranda H, Cabal-Yepez E & Romero-Troncoso R J, Nonlinear observer-based control for an active rectifier, *J Sci Ind Res*, **70** (2011) 1017-1025.
- 33 Saari H, Caron B & Tadjine M, On the design of discrete time repetitive controllers in closed loop configuration", *AUTOMATIKA*, **51** (2010) 333-344.
- 34 Yildirim S, A proposed neural internal model control for robot manipulators, *J Sci Ind Res*, **65** (2006) 713-720.